

Optimizing the Fine Lock Performance of the
Hubble Space Telescope Fine Guidance Sensors

N 93-24723
JUN 1992

David J. Eaton
Richard Whittlesey
Linda Abramowicz-Reed
Robert Zarba

Hughes Danbury Optical Systems, Inc.
100 Wooster Heights Road
Danbury, Connecticut 06810

JUN 1992

15

ABSTRACT

This paper summarizes the on-orbit performance to date of the three Hubble Space Telescope Fine Guidance Sensors (FGS's) in Fine Lock mode, with respect to acquisition success rate, ability to maintain lock, and star brightness range. The process of optimizing Fine Lock performance, including the reasoning underlying the adjustment of uplink parameters, and the effects of optimization are described.

The Fine Lock optimization process has combined theoretical and experimental approaches. Computer models of the FGS have improved understanding of the effects of uplink parameters and fine error averaging on the ability of the FGS to acquire stars and maintain lock. Empirical data have determined the variation of the interferometric error characteristics (so-called "s-curves") between FGS's and over each FGS field of view, identified binary stars, and quantified the systematic error in Coarse Track (the mode preceding Fine Lock). On the basis of these empirical data, the values of the uplink parameters can be selected more precisely.

Since launch, optimization efforts have improved FGS Fine Lock performance, particularly acquisition, which now enjoys a nearly 100 percent success rate. More recent work has been directed towards improving FGS tolerance of two conditions that exceed its original design requirements. First, large amplitude spacecraft jitter is induced by solar panel vibrations following day/night transitions. This jitter is generally much greater than the FGS's were designed to track, and while the tracking ability of the FGS's has been shown to exceed design requirements, losses of Fine Lock after day/night transitions are frequent. Computer simulations have demonstrated a potential improvement in Fine Lock tracking of vehicle jitter near terminator crossings.

Second, telescope spherical aberration degrades the interferometric error signal in Fine Lock, but use of the FGS two-thirds aperture stop restores the transfer function with a corresponding loss of throughput. This loss requires the minimum brightness of acquired stars to be about one magnitude brighter than originally planned.

1. INTRODUCTION

The Hubble Space Telescope (HST) Fine Guidance Sensors (FGS's) serve the dual functions of providing an absolute pointing reference to the telescope pointing control system (PCS), and, as a goal, serving as an astrometry instrument. The FGS's have been used extensively since the telescope was launched in April, 1990.

The FGS's are capable of tracking stars in two modes: Coarse Track, and Fine Lock. This paper reviews FGS performance in Fine Lock, the more accurate of the tracking modes, and discusses the methods by which Fine Lock performance has been and is continuing to be improved.

Copyright © Hughes Danbury Optical Systems, Inc. 1992
All or Portions of the Work Discussed herein was
Supported by NASA Marshall Space Flight Center,
Huntsville, Alabama, under contract no. NAS-8-32700,
and by NASA Goddard Space Flight Center, Greenbelt,
Maryland, under contract no. NAS-8-38494.

Section 2 provides an overview of FGS design and function, while Section 3 summarizes on-orbit Fine Lock performance to date. A discussion of the Fine Lock optimization processes is given in Section 4. Finally, Section 5 presents a brief summary.

2. FGS DESCRIPTION

The descriptions of the HST Fine Guidance Sensors in References 1 and 2 are summarized here.

2.1 Optical/Mechanical Description

In the HST, there are four Radial Bay Modules, three of which containing an FGS. An optical schematic is given in Figure 1. Light from the outer portion of the HST field of view, 10 to 14 arcminutes from the optical axis, strikes the FGS pickoff mirror and is collimated and directed through apertures in a pair of star selector servos. The beam then passes through beamsplitters and Koester prisms before reaching four photomultiplier tubes (PMT's). The angular positions of the servos determine which 5 by 5 arcsecond portion of the FGS field of view enters the fieldstops of the PMT's.

2.2 FGS Control and Modes of Operation

The Fine Guidance Electronics (FGE), an electronics box that includes two microprocessors, controls the FGS. The FGE receives commands, accepts pulse trains from the four PMT's, and receives data from the servo encoders. FGE algorithms define a set of complex operating modes. Among the FGE commands are those that set the values of 38 uplink parameters, which are used to adapt the system to specific mission requirements or special operating conditions. The FGE also outputs data, such as PMT counts, servo encoders, and status bits.

The FGS modes relating to acquisition, pointing and tracking are Search, Coarse Track, and Fine Lock. In Search, the servos define a spiral scan of a region of the FGS field of view, until the target star image enters the PMT fieldstops. When the summed output (counts) of the four PMT's exceeds a commanded threshold, the FGS autonomously terminates Search Mode and enters Coarse Track. In Coarse Track, the FGE commands the servos to move the images of the target star in circular paths (called nutation circles) about the PMT fieldstops. The Coarse Track algorithm monitors the total output of the four PMT's and adjusts the centers of the nutation circles until the circles are centered on the fieldstops.

About 70 percent of all observations are done with the guidance FGS's in Coarse Track mode. The remaining observations require the low jitter provided by Fine Lock. Also, to achieve the positional accuracy required by astrometry observations, Fine Lock is necessary.

While Search and Coarse Track modes use the sum of the outputs from all four PMT's as feedback, Fine Lock uses the PMT's as part of a unique Koester prism interferometer (Figure 2). Fine Lock creates a two-axis position control loop that drives the interferometer to null.

To acquire a star in Fine Lock, the FGS line of sight, as determined by the servo positions, is offset from the center of the Coarse Track nutation circle, the center being the best estimate of the star position in Coarse Track. The servos are then stepped along a straight path toward the star (Figure 3). When the servo positions are within about 0.040 arcseconds of interferometer null along an axis, the error signal increases above a preset threshold, and the FGE reduces the speed of the "walk" toward the star. For each axis, if the error signal exceeds the threshold for 3 consecutive samples, that axis is "locked"; that is, closed-loop operation of the servos is initiated, with the interferometric error signal as position feedback. When both axes are locked, the Fine Lock acquisition is complete, and the servo loop acts to maintain the pointing error at null.

3. FGS ON-ORBIT PERFORMANCE

References 2 and 3 reported on-orbit FGS performance, and compared that performance to the original design requirements. FGS performance that is related to Fine Lock acquisition, pointing and tracking is summarized below.

3.1 Fine Lock Acquisitions

The original FGS design requirements included a star brightness range of 9 to 14.5 Mv for guidance and 10 to 17 Mv for astrometry. However, as a result of spherical aberration in the telescope, it is necessary to operate the FGS's with the two-thirds aperture stop in place. While this aperture stop improves the Fine Lock error signal, there is a reduction in the number of photons reaching the PMT's for a given star, and, consequently, the limiting star magnitude is one Mv brighter than originally expected.

Operating within the above brightness constraint, the FGS's have accomplished a high success rate in Fine Lock acquisitions, at least 93 percent in both guidance and astrometry.

3.2 Moving Target Tracking

Due to solar panel vibrations following day/night transitions, the spacecraft jitter velocities and accelerations greatly exceed the original FGS specifications. In Fine Lock, the FGS'S maintain lock through about 70 percent of the transitions.

3.3 Dynamic Pointing Error

Dynamic pointing error refers to pointing errors that vary over an observation interval and degrade the point spread function of the target image. Dynamic pointing error of the HST has been shown to meet the original requirement of 7 milliarc-seconds, rms, during quiescent periods, with the guidance FGS's in Fine Lock. This result indicates indirectly that the FGS's contribution to dynamic pointing error meets requirements.

Temperature-induced deformations of internal FGS components affect the dynamic pointing error over long-term observations. Temperature measurements of those FGS components that affect pointing stability have indicated that long-duration dynamic pointing error would also meet requirements, were it not for disruptions from vehicle jitter near terminator crossings.

4. FGS FINE LOCK ON-ORBIT OPTIMIZATION

4.1 Optimization Methods

The Fine Lock optimization process has combined theoretical and experimental approaches. Computer analyses and simulations have improved understanding of the effects of uplink parameters and other commands and have been used to evaluate proposed changes. In addition, certain measurements have characterized the on-orbit environment and have been essential to improving FGS performance.

4.1.1 Computer Analyses and Simulations

Several computer-based FGS analyses and simulations have been used before and after launch of the HST.

An analysis of the probability of successful acquisition in Fine Lock, as a function of the relevant uplink

parameters (such as acquisition threshold, s-curve scale factor, walk duration and step size), s-curve degradation, star brightness, PMT responsivity and noise, background illumination, the length of the PMT averaging interval, and spacecraft drift rate, was exercised extensively before and during the ground testing of the FGS's. This analysis helped establish baseline parameter settings, which have been changed only slightly to adapt the FGS's to on-orbit conditions, and verified changes that were made to FGE firmware before launch.

Monte Carlo FGS simulations were used to evaluate probabilities of Fine Lock acquisition and Fine Lock maintenance. The acquisition simulation verified the analysis described in the preceding paragraph. The loss-of-lock simulation was used to set uplink parameters and verify changes to the FGE firmware. It also showed that loss of lock would not occur unless precipitated by a large disturbance, cosmic rays in particular. On-orbit, cosmic rays have not been a problem, but losses of lock are caused by the South Atlantic Anomaly and vehicle jitter following day/night transitions.

A detailed FGS simulation/emulation was developed and used extensively throughout the development, ground testing and on-orbit optimization of the FGS's. This software combines simulations of FGS optics, servo mechanics and electronics, and the HST Pointing Control System with a complete emulation of the FGE firmware. The simulation/emulation is used for problems that require a highly accurate FGS model, but, due to its computational speed, is not suitable for long runs or large numbers of runs, as in Monte Carlo simulations.

Finally, a simple, fast-running Fine Lock simulation, described in more detail in Section 4.3.2, was developed to investigate optimization of FGS tracking performance. Frequency-domain analyses, based on the model used in this simulation, were also developed.

4.1.2 Measured Data

Collecting and cataloging on-orbit data have been essential to the process of optimizing Fine Lock. These data have included s-curves as functions of FGS number and field position, Coarse Track bias errors, vehicle jitter resulting from terminator crossings (day/night transitions), the identification of binary stars, the effects of the South Atlantic Anomaly, sky background illumination, and PMT output and noise vs. star brightness.

4.2 Fine Lock Acquisition Optimization

The most common Fine Lock acquisition failures fall into two general categories. First, the acquisition threshold may fail to be exceeded three samples in succession, and, as a consequence, closed-loop operation may not be initiated in one or both axes. Second, the threshold may be exceeded by noise ("false lock") before the lobes of the s-curve are reached, and the star will drift out of the PMT fieldstops and be lost. When acquisition uplink parameters are adjusted, the probability of one type of failure will increase, while the other decreases. A compromise is therefore required.

4.2.1 Uplink Parameter Adjustment

A block diagram of Fine Lock acquisition (Figure 4) shows the most important acquisition uplink parameters. The Fine Error Signal (FES) is calculated at the end of a PMT averaging period as follows:

$$FESX = K0X + K1X*QX \quad (1)$$

$$FESY = K0Y + K1Y*QY, \quad (2)$$

where $K0X$, etc., are uplink parameters and QX and QY are calculated from the PMT counts, AX , BX , AY , and BY from the equations

$$QX = (AX - BX - DIFFX)/(SUMX) \quad (3)$$

$$QY = (AY - BY - DIFFY)/(SUMY). \quad (4)$$

The quantities DIFFX, DIFFY, SUMX and SUMY are the initial sums and differences of the PMT counts measured over an interval at the beginning of Fine Lock mode, before the "walk", and held constant until Fine Lock is terminated.

A plot of QX or QY against true FGS pointing error has the shape of the "s-curve" shown in Figure 2b. (The DIFF terms in equations 3 and 4 are assumed to be zero in Figure 2b.) With reference to Figure 2a, a true pointing error of zero (interferometer null) corresponds to an incoming wavefront being parallel to the face of the Koester prism. At null, each PMT receives equal illumination, and the output of PMT A equals the output of PMT B; therefore QX or QY is zero. For a small wavefront tilt (true pointing error slightly nonzero), constructive and destructive interference is set up in the Koester prism, such that the illumination entering one PMT is increased and illumination entering the other PMT is decreased. Thus the difference (A - B) and consequently QX or QY are nonzero. For larger pointing errors, interference no longer occurs and the PMT outputs are about equal. QX and QY are nominally zero for pointing errors greater than about 0.04 arcsecond.

In a nominal configuration, the PMT counts are averaged over 0.025 second and the servo commands are updated at the same rate. If PMT averaging is commanded, this period is increased by a factor that is a power of two. For example, with "two-sample averaging", the PMT averaging and servo update interval is doubled to 0.05 second. PMT averaging is used to reduce PMT photon noise with dim stars during astrometry acquisitions.

The most important acquisition parameters are K1X, K1Y and KZ. The first two scale the s-curve to compensate for variations in the s-curve shape and are selected to calibrate the FES; that is, the slope of the scaled s-curve is adjusted to unity. KZ sets the acquisition threshold. Pre-launch analyses, Monte Carlo simulations and tests established the best value of KZ to be 60 percent of the scaled s-curve peak. However, on-orbit, it was soon found that 50 percent resulted in a significantly improved acquisition success rate. Since sky background illumination and the resulting PMT noise were smaller than assumed prior to launch, the threshold could be lowered without a risk of "false lock".

In general, KZ has been held constant, and K1X and K1Y have been adjusted to correct the s-curves, as much as possible, to a "standard" shape. Different FGS's are assigned different values, but the adjustment for star brightness is small. Since the s-curves vary over the FOV of an FGS, K1X and K1Y should ideally vary over the FOV as well. However, for practical reasons, this is not done; rather, the values of K1X and K1Y are determined for the s-curve having the smallest modulation.

Parameters K0X and K0Y can correct bias in the s-curves; however, this correction has not been made ($K0X = K0Y = 0$), since the bias is generally not known a priori. The limiters K3X and K3Y have been set slightly above the highest s-curve peak to clip noise. These parameters do not affect Fine Lock acquisitions, as long as the products, $K1X*K3X$ and $K1Y*K3Y$ are greater than KZ.

The geometry of the Fine Lock walk is determined by parameters KD (step size), K10 (servo rate command gain), K05 (total number of steps) and KB (offset of start point from the center of the Coarse Track circle). Together, KD and K10 determine the actual step size, which is usually different from the value of KD itself. Selection of KD and K10 is another compromise. A large step size (rapid walkdown) is desirable, as it reduces susceptibility to noise; however, if the step is too large, too few samples of the FES will be taken in the lobes of the s-curves, and the peaks may be missed. The current values of K10 and KD are selected to give an actual step size of about 0.006 arcseconds, per axis. This step size is less than the pre-launch value of 0.009 arcsecond and reflects the fact that PMT noise on-orbit is lower than expected, as noted above. The walkdown rate relative to the star also depends on spacecraft drift; however, drift rate is not known beforehand, and is therefore not

compensated.

The starting and ending points of the Fine Lock walk are determined by KB, K05, and the actual step size established by K10 and KD. Knowledge of the Coarse Track bias error, the difference between the steady-state center of the Coarse Track nutation circle and the Fine Lock null, is necessary to set KB and K05. During early attempts to acquire stars in Fine Lock, shortly after HST launch, it was observed that FGS number 1 would frequently fail to acquire. Data analysis revealed a large Coarse Track bias in the x axis, and it was necessary to increase KB from about 0.6 arcsecond to about 1 arcsecond to compensate. It was also necessary to increase K05 to prevent the walk from terminating before the null was reached.

It is also possible to reverse the direction of the walk, i. e., start the walk in the third rather than first quadrant, by changing the signs of KB and KD. This capability may help acquisitions with certain types of asymmetric s-curves, but it has not yet been utilized.

4.2.2 The Effect of the South Atlantic Anomaly on Acquisitions

The charged particles present in South Atlantic Anomaly (SAA) increase PMT counts. Consequently, the PMT noise level and the probability of false lock increase. While partial compensation may be achieved by increasing KZ, in practice acquisitions in the SAA are avoided when observations are planned.

4.3 Optimization of the FGS's Ability to Maintain Fine Lock

After Fine Lock Acquisition is complete, the FGS, under FGE control, functions as a position control system (the "Fine Lock Loop"), with feedback from the Koester prism interferometer. This control system has a closed-loop bandwidth of about 9 Hz (-3 db), when the interferometer error is in the linear region of the s-curve, the relevant uplink parameters are set at nominal values, and PMT averaging is not in effect. Since the error characteristic is nonlinear, a large disturbance to the position loop can potentially create errors beyond a lobe of the s-curve, and Fine Lock can be lost. In practice, the only disturbances that cause loss of Fine Lock are 1) vehicle jitter caused by terminator crossings (solar panel vibrations), 2) the South Atlantic Anomaly, and 3) vehicle slews, with rate feedforward provided to the FGS's by the PCS. The success of vehicle slews depends on the quality of the feedforward commands and is not discussed further in this paper.

4.3.1 Tracking Vehicle Jitter Caused by Terminator Crossings

A simplified block diagram of one axis of the Fine Lock Loop is shown in Figure 5. The dynamic characteristics of the system, including bandwidth, are controlled by several uplink parameters: K1X, K1Y, K3X, K3Y, K13 (proportional gain), K14 (integral gain), K15 (differential gain) and K31 (integral limit). Note that the FES is calculated in the same way as it is during acquisitions (Equations 1-4). Potentially, tracking through terminator disturbances can be improved by adjusting these parameters.

In general, parameter adjustments that increase the bandwidth of the Fine Lock Loop should improve tracking of spacecraft jitter; however, FGS noise equivalent angle (NEA), servo motion in response to PMT photon noise, also increases with bandwidth. Thus, as in Fine Lock acquisition optimization, adjusting Fine Lock loop parameters involves a compromise.

Since FGS dynamic pointing error, to which NEA is a contributor, has been low, it should be possible to significantly increase the bandwidth of the system and still have acceptable NEA. Furthermore, depending on the frequency content of the solar panel jitter, some parameter adjustments are more effective than others in improving tracking with an equal increase in NEA.

4.3.2 Predictions From Simulations

To determine the effects of uplink parameters on tracking, a simple computer simulation of one axis of the Fine Lock loop was programmed. This simulation basically follows the block diagram in Figure 5. The following assumptions and approximations were made:

1. PMT integration was approximated by averaging the pointing errors at the start and end of an integration period;
2. The Pointing Control System (PCS) was not included in the simulation;
3. The s-curve was approximated by a single cycle of a sine wave;
4. The star selector servo was modelled as an ideal rate servo (integrator); and
5. Quantization effects in the FGE were not included.

Initial simulations were run with a spacecraft jitter of 0.1 arcsecond amplitude (zero to peak) and 0.6 Hz frequency. Jitter of this amplitude is sometimes observed near a terminator crossing. Furthermore, a solar panel vibration mode of about 0.6 Hz is frequently in evidence in the jitter.

The simulations showed that increasing the bandwidth of the Fine Lock loop, by increasing the gains K13 (proportional) and/or K14 (integral) reduced the amplitude of the steady-state FGS tracking error. (See example in Figure 6.) Furthermore, certain parameter adjustments, particularly increased integral gain (K14), yielded lower tracking error for the same increase in NEA. Table 1 compares the effects of K13 and K14 on tracking error and NEA. The reason K14 was effective was that it boosted the open-loop gain at low frequencies (relative to the system bandwidth of 9 Hz, without increasing the crossover frequency as much as other parameter adjustments did. This gain increase reduced the tracking error for low frequencies, including 0.6 Hz.

Fine Lock tracking performance with two-sample (0.05 second) PMT averaging, null by-pass on, was also simulated. (When null by-pass is on, the servos move according to their last rate command update during the PMT averaging period.) PMT averaging has the effect of "time scaling" the Fine Lock loop in proportion to the duration of the averaging period. Thus, the 8-10 Hz Fine Lock loop, without PMT averaging, becomes a 4-5 Hz loop with two-sample averaging, and tracking performance is progressively degraded as the averaging period is increased. As shown in Table 2, it was necessary to reduce the jitter amplitude to allow the FGS to stay in lock at all. Note that K14 was not as effective in reducing the tracking error as in Table 1, since 0.6 Hz is not as low a frequency relative to the bandwidth.

The values of differential gain, K15, that can be commanded were found to be too small to significantly affect tracking performance.

4.3.3 Experimental Results

The FGS's were operated with the integral gain, K14, increased to eight times its nominal value, on several occasions in late 1991 and early 1992. Since these experiments were not controlled, no definite conclusions can be drawn. However, a high percentage of the terminator crossings resulted in loss of Fine Lock, so there was no apparent improvement from increasing K14. Data from these tests is being analyzed to determine why no improvement was obtained.

Two losses of lock with increased K14 have been analyzed to date. In the first example, the vehicle jitter,

obtained from gyro data sampled at 40 Hz, was seen to be dominated by a frequency near 1.4 Hz, rather than 0.6 Hz (Figure 7). Thus, the conclusions of the preceding section, which were based on 0.6 Hz jitter, do not apply to this case. In the second example (Figure 8), 0.6 Hz was the dominant frequency, but the amplitude was very large, up to 0.25 arcsecond. Note that the FGS was apparently able to track 0.6 Hz jitter with an amplitude over 0.20 arcsecond, but not 0.25 arcsecond. Therefore, it should have been able to track more "typical" jitter, having an amplitude of 0.10 arcsecond. Since there was no experimental control, we cannot conclude that increasing K14 was ineffective in this case.

Further analysis of jitter data is necessary to determine what terminator jitter looks like. Once this is done, the problem of determining the best settings of the Fine Lock Loop parameters can be re-visited.

4.3.4 Effects of the South Atlantic Anomaly (SAA) on Loss of Fine Lock

When the HST is in the SAA, charged particles increase the outputs of the FGS PMT's. The increases may be equal in all PMT's, or unequal, depending on how well each PMT is shielded from the particles. With reference to Equations (1-4), if a Fine Lock acquisition occurs in the SAA, the "SUM" quantities will be larger than normal, and the gain and bandwidth of the Fine Lock Loop will be reduced. Furthermore, one or both of the "DIFF" quantities may be large, leading to a large bias in the FES when the HST leaves the SAA. The bandwidth reduction and the bias increase the chances of a loss of lock caused by disturbances, such as spacecraft jitter.

If a Fine Lock Acquisition occurs outside of the SAA, the "SUM" and "DIFF" terms are nominal. However, if the HST subsequently enters the SAA, the photon noise level increases. There may also be a bias in the FES if the PMT's are not affected equally. Again, the chances for a loss of lock are increased.

Observations are scheduled to avoid operation in the SAA.

5. SUMMARY

The HST Fine Guidance Sensors have been performing well on-orbit and have met or performed better than original requirements relating to Fine Lock acquisitions, moving target tracking, and dynamic pointing error. A combined theoretical and experimental approach has been used to optimize Fine Lock performance. Prior to launch, analyses and simulations of Fine Lock, as well as ground tests, established the best estimates for Fine Lock uplink parameters. Since launch, further analyses, simulations and measured data have been used to refine these estimates. Table 3 lists the Fine Lock uplink parameters, with their before-launch and current values.

Particular attention has been given to the effects of telescope spherical aberration and the effects of spacecraft jitter from terminator crossings. Measurements of the Fine Lock error characteristics (s-curves) have been used to set error gains and acquisition thresholds. The on-board two-thirds aperture filter has reduced the effects of spherical aberration on the s-curves; however, the loss of throughput to the PMT's requires that the minimum brightness of acquired stars be about one magnitude brighter than originally planned. As shown in Table 3, the values of interferometer parameters (K1X, K1Y, K3X, and K3Y) are set on the basis of measured s-curves, which vary between FGS's and over the field of view of an FGS.

While FGS tracking capability has been better than originally required, computer simulations have demonstrated a potential improvement in Fine Lock tracking of vehicle jitter near terminator crossings, by adjustment of the control loop gains (K13, K14 and K15). Jitter data is presently being reviewed to establish the amplitude and frequency content of the jitter, so that the best parameter values may be selected.

6. ACKNOWLEDGEMENTS

The work reported here was sponsored by NASA Marshall Space Flight Center, Huntsville, Alabama, under contract no. NAS-8-32700, and by NASA Goddard Space Flight Center, Greenbelt, Maryland, under contract no. NAS-8-38494.

A very large number of individuals from Hughes Danbury Optical Systems, NASA, Lockheed Missiles and Space Company, and other organizations contributed to the design, fabrication, calibration, testing and operation of the HST Fine Guidance Sensors. The authors wish to acknowledge the extensive work of these contributors and would like to thank the organizations involved for the privilege of presenting this paper. In particular, we would like to thank Greg Andersen and Theresa Gaston of Jackson and Tull, Inc., and Darrell Story of the University of Texas, for their technical contributions. We would also like to thank Geralyn Fischer for her assistance in preparing the manuscript.

7. REFERENCES

1. G. S. Nurre, S. J. Anhouse, and S. N. Gullapalli, Hubble Space Telescope Fine Guidance Sensor Control System, SPIE Technical Symposium, Orlando, Florida, March, 1989.
2. D. Eaton, et al., On-Orbit Performance of the Hubble Space Telescope Fine Guidance Sensors, Space Optics for Astrophysics, Williamsburg, Virginia, November 18-19, 1991.
3. D. Eaton, et al., Acquisition, Pointing, and Tracking Performance of the Hubble Space Telescope Fine Guidance Sensors, SPIE Aerospace Sensing Symposium, Orlando, Florida, April 20-24, 1992.

Table 1. Simulated FGS Fine Lock tracking performance, no PMT averaging; shows tracking error as a function of parameters K_{13} and K_{14}

UPLINK PARAMETERS		AMPLITUDE OF STEADY-STATE POINTING ERROR (M.A.S.)	NEA** INCREASE WITH RESPECT TO NOMINAL (PERCENT)
K_{13}	K_{14}		
NOMINAL	NOMINAL	LOCK LOST*	0
NOMINAL	2 X NOMINAL	16.5°	7
NOMINAL	5 X NOMINAL	7°	30
NOMINAL	8 X NOMINAL (MAX. COMMANDABLE)	4	57
.8 X NOMINAL	8 X NOMINAL	4	52
1.5 X NOMINAL	1.5 X NOMINAL	12	42
2 X NOMINAL	2 X NOMINAL	8	98

*PLOTTED IN FIGURE 6.

**NOISE EQUIVALENT ANGLE.

INPUT JITTER: 100 M.A.S. AMPLITUDE, 0.6 HZ

Table 2. Simulated FGS Fine Lock tracking performance, two-sample PMT averaging; shows tracking error as a function of parameters K_{13} and K_{14}

UPLINK PARAMETERS		AMPLITUDE OF STEADY-STATE POINTING ERROR (M.A.S.)	NEA** INCREASE WITH RESPECT TO NOMINAL (PERCENT)
K_{13}	K_{14}		
NOMINAL*	NOMINAL*	LOCK LOST	0
NOMINAL	2 X NOMINAL	LOCK LOST	7
NOMINAL	5 X NOMINAL	14	30
NOMINAL	10 X NOMINAL	7	79
NOMINAL	15 X NOMINAL	4.5	160
1.5 X NOMINAL	1.5 X NOMINAL	14	42
2 X NOMINAL	2 X NOMINAL	9	98

*NOMINAL SETTINGS ARE ONE-HALF THE NO-AVERAGING VALUES.

**NOISE EQUIVALENT ANGLE.

INPUT JITTER: 50 M.A.S. AMPLITUDE, 0.6 HZ

Table 3. Summary of Fine Lock uplink parameters and their values

PARAMETER	NAME	VALUE PRIOR TO HST LAUNCH (LSB'S)	CURRENT VALUES (LSB'S)
K_{ax}, K_{ay}	Interferometer bias	0	0
K_{1x}, K_{1y}	Interferometer scale factor	Based on measured s-curves	Based on measured s-curves
K_{3x}, K_{3y}	Interferometer limit		
K_8	Radial offset for start of Fine Lock walk	566	Based on measured Coarse Track bias
K_9	Step size during walk	226**	162**
K_{10}	Gain during walk	384	384
K_{11}	Acquisition threshold	100	88
K_{12}	Proportional gain	432	432*
K_{14}	Integral gain	173	173*
K_{15}	Differential gain	0	0*
K_{31}	Integral limit	411	411

*Being investigated for tracking improvement.

**No PMT averaging.

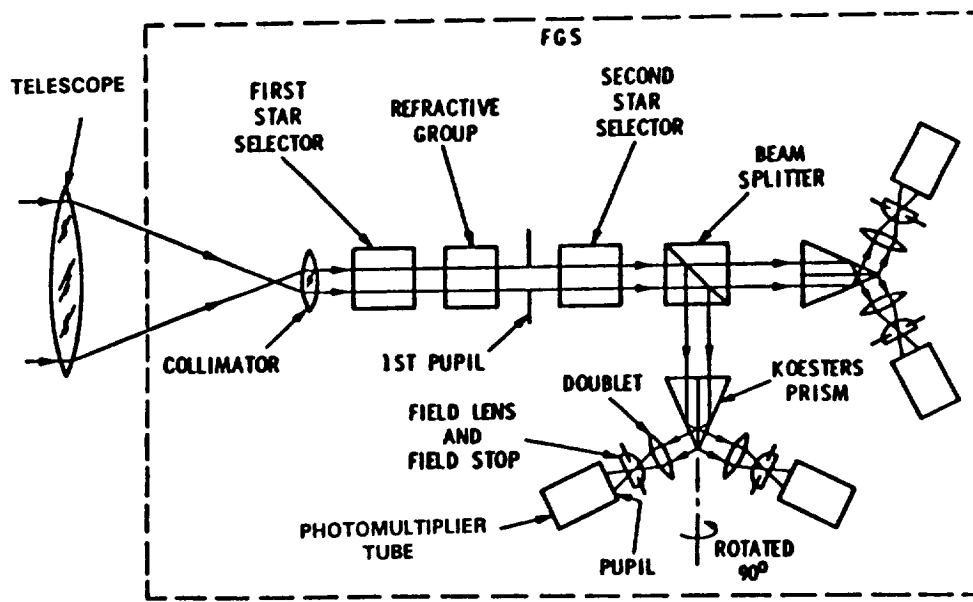


Figure 1. Simplified FGS schematic, showing star selector servos, Koester's prisms and photomultiplier tubes

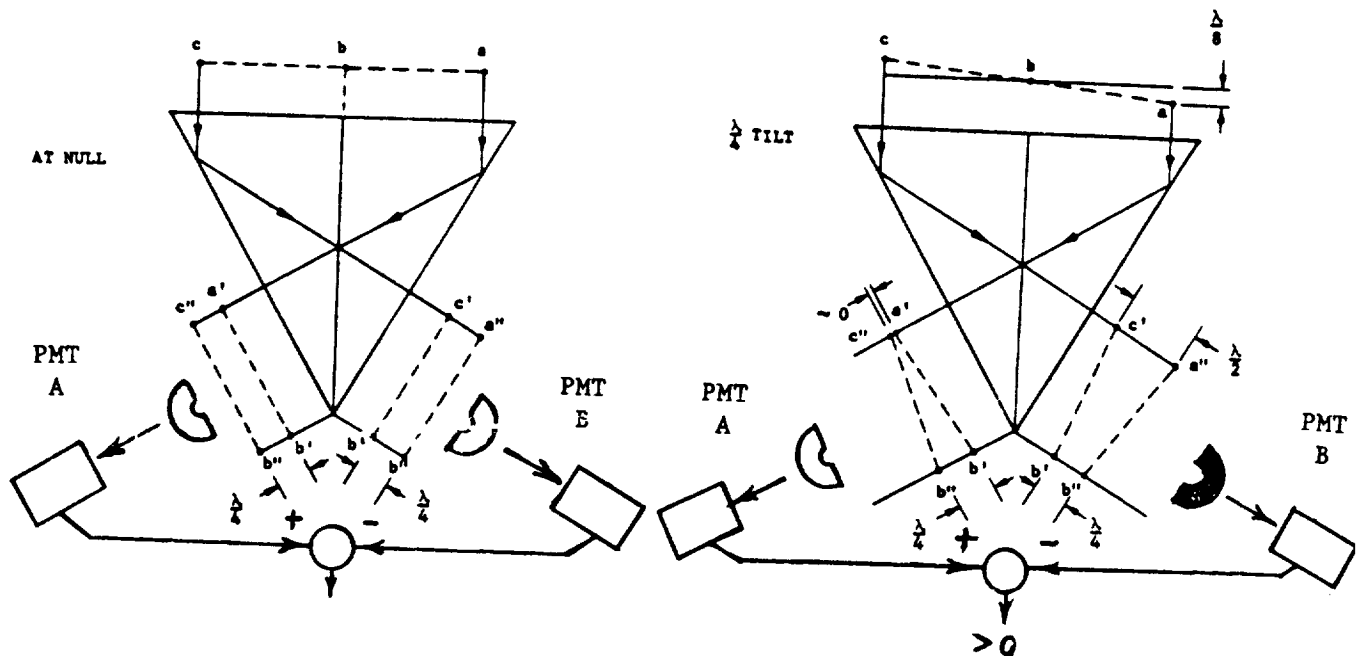


Figure 2a. Koester prism interferometer. Interferometer null is obtained when the incoming wavefront is parallel to the face of the prism and the PMTs are equally illuminated

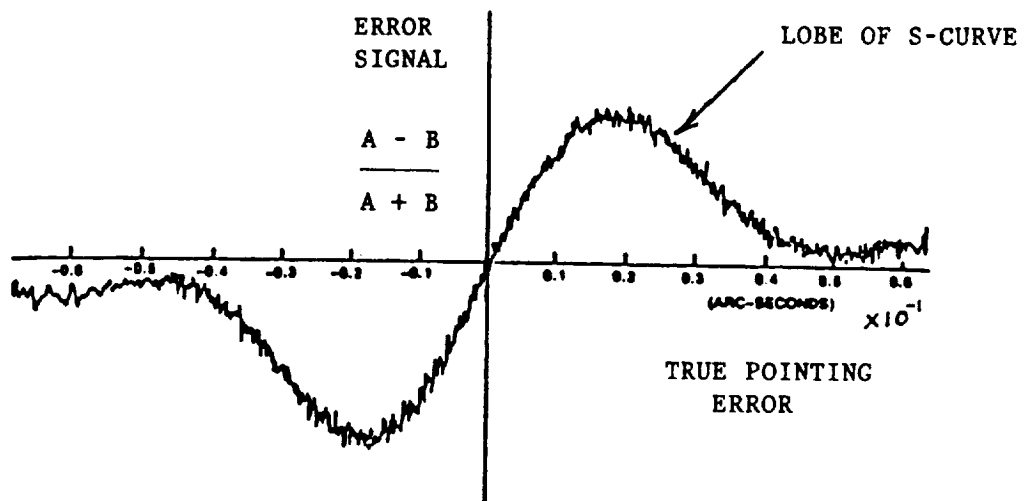


Figure 2b. Measured FGS interferometer characteristic. The "s-curve" is a plot of measured pointing error vs. true pointing error

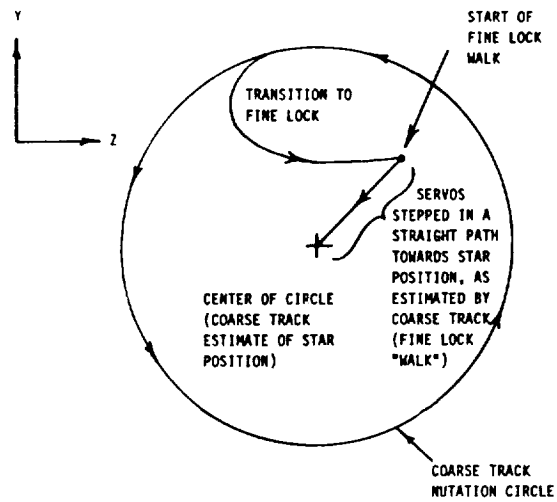


Figure 3. Transition from Coarse Track to Fine Lock
Plot of FGS line of sight as determined by star selector servos

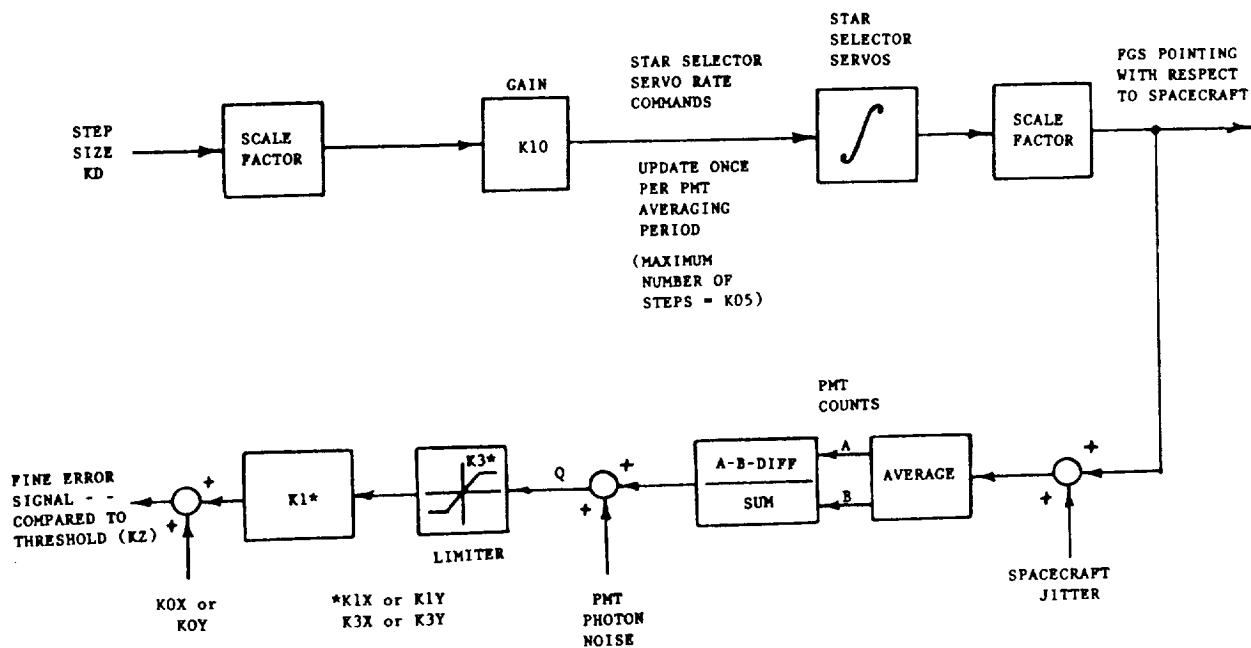


Figure 4. Simplified Fine Lock acquisition block diagram
(one axis)

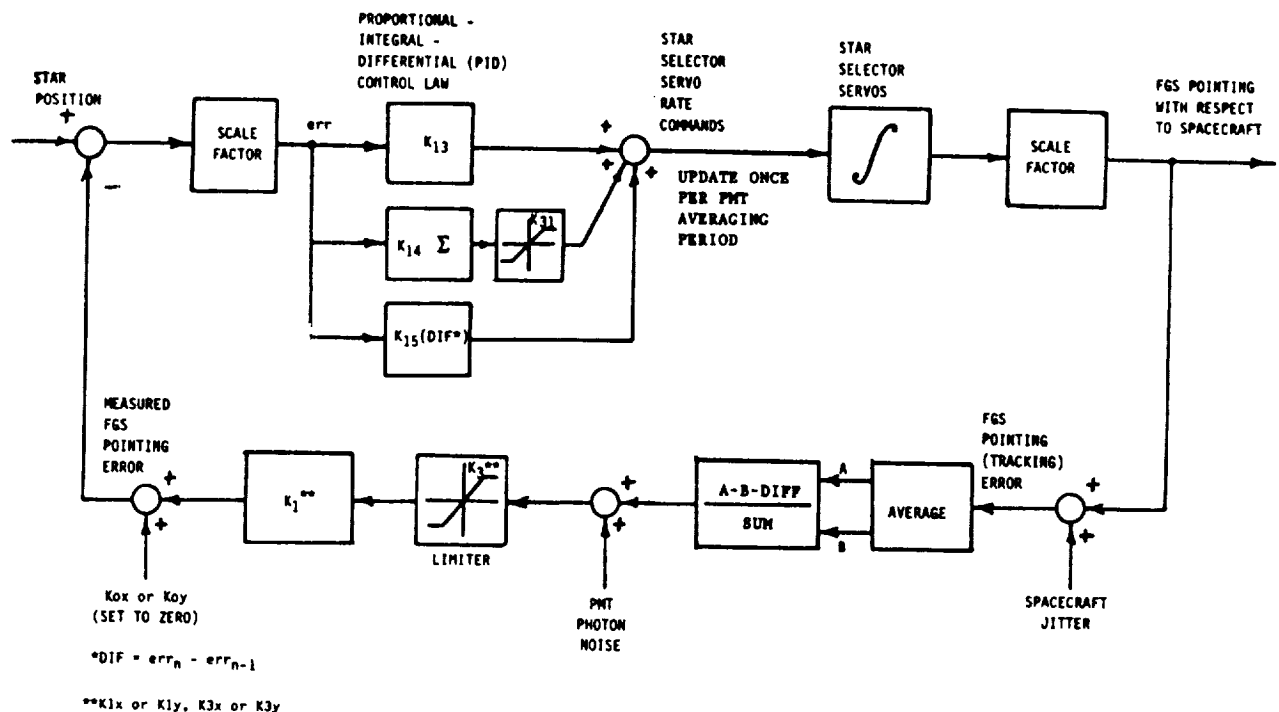


Figure 5. Simplified block diagram of one axis of the Fine Lock position loop

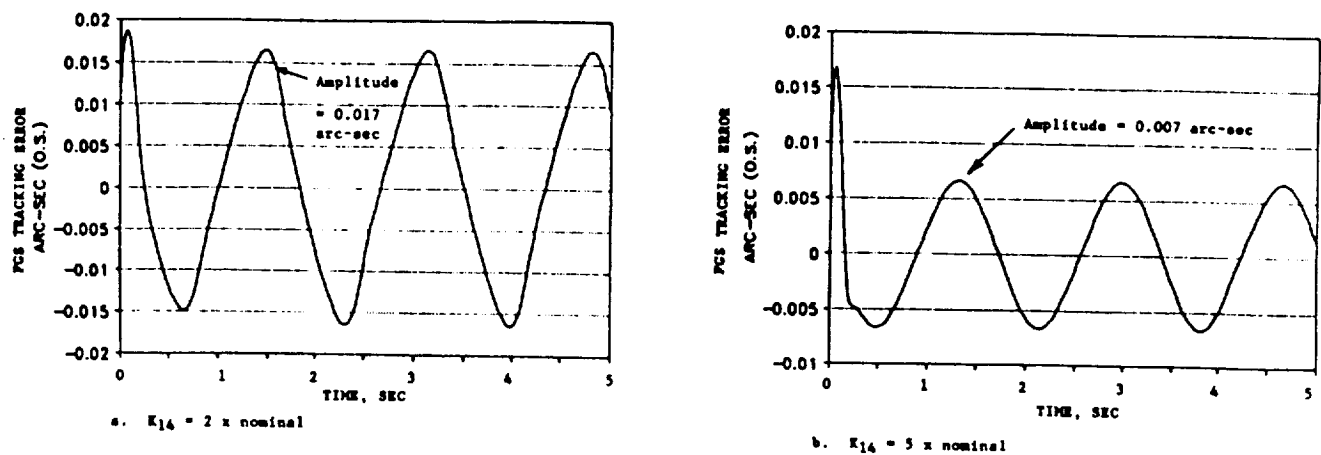


Figure 6. Simulations showing the sensitivity of FGS tracking error to increased bandwidth of the Fine Lock loop (via parameter K₁₄)
 Spacecraft jitter: 0.1 arc-second (object space) amplitude (zero-peak), 0.6 hz

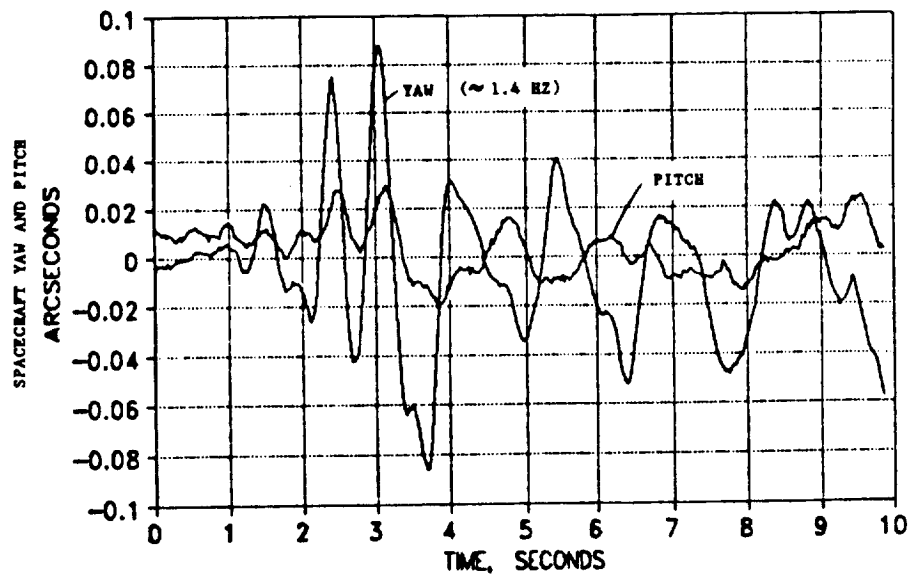


Figure 7. First example of spacecraft jitter from solar panel vibrations near the terminator

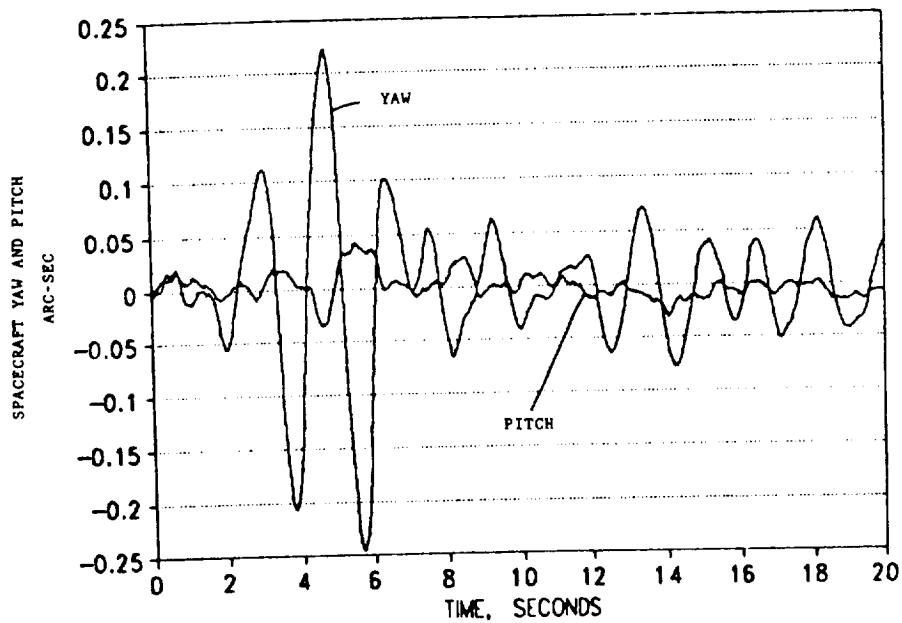


Figure 8. Second example of spacecraft jitter from solar panel vibrations near the terminator

